

1 **Nitrogen Fixation in Arctic Coastal Waters (Qeqertarsuaq, West**
2 **Greenland): Influence of Glacial Melt on Diazotrophs, Nutrient**
3 **Availability, and Seasonal Blooms**

4 Schlangen Isabell¹, Leon-Palmero Elizabeth^{1,2}, Moser Annabell¹, Xu Peihang¹, Laursen Erik¹, and
5 Löscher Carolin R.^{1,3}

6 ¹Nordceee, Department of Biology, University of Southern Denmark, Campusvej 55, 5230 Odense M, Denmark

7 ²Department of Geosciences, Princeton University, Princeton, New Jersey

8 ³DIAS, University of Southern Denmark, Odense, Denmark

9 **Correspondence:** Carolin R. Löscher (cloescher@biology.sdu.dk)

10 **Abstract.** The Arctic Ocean is undergoing rapid transformation due to climate change, with decreasing sea ice contributing
11 to a predicted increase in primary productivity. A critical factor determining future productivity in this region is the
12 availability of nitrogen, a key nutrient that often limits biological growth in Arctic waters. The fixation of dinitrogen (N₂)
13 gas, a biological process mediated by diazotrophs, not only supplies new nitrogen to the ecosystem but also plays a
14 central role in shaping the biological productivity of the Arctic. Historically it was believed to be limited to oligotrophic
15 tropical and subtropical oceans, Arctic N₂ fixation has only garnered significant attention over the past decade, leaving
16 a gap in our understanding of its magnitude, the diazotrophic community, and potential environmental drivers. In this
17 study, we investigated N₂ fixation rates and the diazotrophic community in Arctic coastal waters, using a combination of
18 isotope labeling, genetic analyses and biogeochemical profiling, in order to explore its response to glacial meltwater,
19 nutrient availability and its impact on primary productivity. Here we show N₂ fixation rates ranging from 0.16 to 2.71 nmol
20 N L⁻¹ d⁻¹, to be notably higher than those observed in many other oceanic regions, suggesting a previously unrecognized
21 significance of N₂ fixation in these high-latitude waters. The diazotrophic community is predominantly composed of
22 UCYN-A. We found highest N₂ fixation rates co-occurring with maximum chlorophyll *a* concentrations and primary
23 production rates at a station in the Vaigat Strait close impacted by glacier meltwater inflow, possibly providing otherwise
24 limiting nutrients. Our findings illustrate the importance of N₂ fixation in an environment previously not considered
25 important for this process and provide insights into its response to the projected melting of the polar ice cover.

27 **1 Introduction**

28 Nitrogen is a key element for life and often acts as a growth-limiting factor for primary productivity (Gruber and Sarmiento,
29 1997; Gruber, 2004; Gruber and Galloway, 2008). Despite nitrogen gas (N₂) making up approximately 78% of the
30 atmosphere, it remains inaccessible to most marine life forms. Diazotrophs, which are specialized bacteria and archaea,
31 have the ability to convert N₂ into biologically available nitrogen, facilitated by the nitrogenase enzyme complex carrying
32 out the process of

35 biological nitrogen fixation (N_2 fixation) (Capone and Carpenter (1982)). Despite the fact that these organisms are highly
36 specialized and N_2 fixation is energetically demanding, the ability to carry out this process is widespread amongst
37 prokaryotes. However, it is controlled by several factors such as temperature, light, nutrients and trace metals such as iron
38 and molybdenum (Sohm et al., 2011; Tang et al., 2019). Oceanic N_2 fixation is the major source of nitrogen to the marine
39 system (Karl et al., 2002; Gruber and Sarmiento, 1997), thus, diazotrophs determine the biological productivity of our
40 planet (Falkowski et al. (2008)), impact the global carbon cycle and the formation of organic matter (Galloway et al., 2004;
41 Zehr and Capone, 2020). Traditionally it has been believed that the distribution of diazotrophs was limited to warm and
42 oligotrophic waters (Buchanan et al., 2019; Sohm et al., 2011; Luo et al., 2012) until putative diazotrophs were identified
43 in the central Arctic Ocean and Baffin Bay (Farnelid et al., 2011; Damm et al., 2010). First rate measurements have been
44 reported for the Canadian Arctic by Blais et al. (2012) and recent studies have reported rate measurements in adjacent seas
45 (Harding et al., 2018; Sipler et al., 2017; Shiozaki et al., 2017, 2018), drawing attention to cold and temperate waters as
46 significant contributors to the global nitrogen budget through diverse organisms.

47 N_2 fixation is performed by diverse group of cyanobacteria as well as by non-cyanobacteria diazotrophs (NCDs). UCYN-
48 A has been described as the dominant active N_2 fixing cyanobacterial diazotroph in arctic waters (Harding et al. (2018)),
49 while other cyanobacteria have only occasionally been reported (Diez et al., 2012; Fernández-Méndez et al., 2016; Blais et
50 al., 2012). Recent studies found that the majority of the arctic marine diazotrophs are NCDs and those may contribute
51 significantly to N_2 fixation in the Arctic Ocean (Shiozaki et al., 2018; Fernández-Méndez et al., 2016; Harding et al., 2018;
52 Von Friesen and Rie- mann, 2020). Still, studies on the Arctic diazotroph community remain scarce, leaving Arctic
53 environments poorly understood regarding N_2 fixation. Shao et al. (2023) note the impossibility of estimating Arctic N_2
54 fixation rates due to the sparse spatial coverage, which currently represents only approximately 1 % of the Arctic Ocean.
55 Increasing data coverage in future studies will aid in better constraining the contribution of N_2 fixation to the global oceanic
56 nitrogen budget (Tang et al. (2019)).

57 The Arctic ecosystem is undergoing significant changes driven by rising temperatures and the accelerated melting of sea ice,
58 a trend predicted to intensify in the future (Arrigo et al., 2008; Hanna et al., 2008; Haine et al., 2015). These climate-driven
59 shifts have stimulated primary productivity in the Arctic by 57 % from 1998 to 2018, elevating nutrient demands in the
60 Arctic Ocean (Ardyna and Arrigo, 2020; Arrigo and van Dijken, 2015; Lewis et al., 2020). This increase is attributed to
61 prolonged phytoplankton growing seasons and expanding ice-free areas suitable for phytoplankton growth (Arrigo et al.
62 (2008)). However, despite these dramatic changes, the role of N_2 fixation in sustaining Arctic primary production remains
63 poorly understood. While recent studies suggest that diazotrophic activity may contribute to nitrogen inputs in polar regions
64 (Sipler et al. (2017)), fundamental uncertainties remain regarding the extend, distribution and environmental drivers of N_2
65 Fixation in the Arctic Ocean. Specifically, it is unclear whether increased glacial meltwater input enhances or inhibits N_2
66 Fixation through changes in nutrient availability, stratification, and microbial community composition. Thus, the question
67 of whether nitrogen limitation will emerge as a key factor constraining Arctic primary production under future climate scenarios
68 remains unresolved. In this study, we investigate the diversity of diazotrophic communities alongside in situ N_2 fixation

69 rate measurements in Disko Bay (Qeqertarsuaq), a coastal Arctic system strongly influenced by glacial meltwater input. By linking
70 environmental parameters to N₂ fixation dynamics, we aim to clarify the role of diazotrophs in Arctic nutrient cycling and
71 assess their potential contribution to sustaining primary production in a changing Arctic. Understanding these processes is
72 essential for refining biogeochemical models and predicting ecosystem responses to future climate change.

73 **2 Material and methods**

74 **2.1 Seawater sampling**

75 The research expedition was conducted from August 16 to 26 in 2022 aboard the Danish military vessel P540 within the
76 waters of Qeqertarsuaq, located in the western region of Greenland (Kalaallit Nunaat). Discrete water samples were
77 obtained using a 10 L Niskin bottle, manually lowered with a hand winch to five distinct depths (surface, 5, 25, 50, and
78 100 m). A comprehensive sampling strategy was employed at 10 stations (Fig. 1), covering the surface to a depth of 100 m.
79 The sampled parameters included water characteristics, such as nutrient concentrations, chl *a*, particulate organic carbon
80 (POC) and nitrogen (PON), molecular samples for nucleic acid extractions (DNA), dissolved inorganic carbon (DIC) as
81 well as CTD sensor data. At three selected stations (3,7,10) N₂ fixation and primary production rates were quantified
82 through concurrent incubation experiments.

83 Samples for nutrient analysis, nitrate (NO₃⁻), nitrite (NO₂⁻) and phosphate (PO₄³⁻) were taken in triplicates, filtered
84 through a 0.22 μ m syringe filter (Avantor VWR® Radnor, Pa, USA) and stored at -20 °C until further analysis.
85 Concentrations were spectrophotometrically determined (Thermo Scientific, Genesys 10S UV-VIS spectrophotometer)
86 following the established protocols of Murphy and Riley (1962) for PO₄³⁻; García-Robledo et al. (2014) for NO₃⁻ & NO₂⁻
87 (detection limits: 0.01 μ mol L⁻¹ (NO₃⁻, NO₂⁻, and PO₄³⁻), 0.05 μ mol L⁻¹ (NH₄⁺)). Chl *a* samples were filtered onto 47 mm
88 ϕ GF/F filters (GE Healthcare Life Sciences, Whatman, USA), placed into darkened 15 mL LightSafe centrifuge tubes
89 (Merck, Rahway, NJ, USA) and were subsequently stored at -20 °C until further analysis. To determine the Chl *a* con-
90 centration, the samples were immersed in 8 mL of 90 % acetone overnight at 5 °C. Subsequently, 1 mL of the resulting
91 solution was transferred to a 1.5 mL glass vial (Mikrolab Aarhus A/S, Aarhus, Denmark) the following day and subjected
92 to analysis using the Trilogy® Fluorometer (Model #7200-00) equipped with a Chl *a* in vivo blue module (Model #7200-
93 043, both Turner Designs, San Jose, CA, USA). Measurements of serial dilutions from a 4 mg L⁻¹ stock standard and 90 %
94 acetone (serving as blank) were performed to calibrate the instrument. In addition, measurements of a solid-state secondary
95 standard were performed every 10 samples. Water (1 L) water from each depth was filtered for the determination of POC
96 and PON concentrations, as well as natural isotope abundance (δ ¹³C POC / δ ¹⁵N PON) using 47 mm ϕ , 0.7 μ m nominal
97 pore size precombusted GF/F filter (GE Healthcare Life Sciences, Whatman, USA), which were subsequently stored at -
98 20 °C until further analysis. Seawater samples for DNA were filtered through 47 mm ϕ , 0.22 μ m MCE membrane filter
99 (Merck, Millipore Ltd., Ireland) for a maximum of 20 minutes, employing a gentle vacuum (200 mbar). The filtered
100 volumes varied depending
101
102
103

104 on the amount of material captured on the filter, ranging from 1.3 L to 2 L, with precise measurements recorded. The filters
105 were promptly stored at -20 °C on the ship and moved to -80 °C upon arrival to the lab until further analysis.
106 To achieve detailed vertical profiles, a conductivity-temperature-depth-profiler (CTD, Seabird X) equipped with
107 supplementary sensors for dissolved oxygen (DO), photosynthetic active radiation (PAR), and fluorescence (Flurometer)
108 was manually deployed.

109 **2.2 Nitrogen fixation and primary production**

110 Water samples were collected at three distinct depths (0, 25 and 50 m) for the investigation of N₂ fixation rates and primary
111 production rates, encompassing the euphotic zone, chlorophyll maximum, and a light-absent zone. Three incubation
112 stations (Fig. 2: station 3, 7, 10) were chosen, in a way to cover the variability of the study area. This strategic sampling
113 aimed to capture a gradient of the water column with varying environmental conditions, relevant to the aim of the study.
114 N₂ fixation rates were assessed through triplicate incubations employing the modified ¹⁵N-N₂ dissolution technique after
115 Großkopf et al. (2012) and Mohr et al. (2010).

116 To ensure minimal contamination, 2.3 L glass bottles (Schott-Duran, Wertheim, Germany) underwent pre-cleaning and
117 acid washing before being filled with seawater samples. Oxygen contamination during sample collection was mitigated by
118 gently and bubble-free filling the bottles from the bottom, allowing the water to overflow. Each incubation bottle received
119 a 100 mL amendment of ¹⁵N-N₂ enriched seawater (98 %, Cambridge Isotope Laboratories, Inc., USA) achieving an
120 average dissolved N₂ isotope abundance (¹⁵N atom %) of 3.90 ± 0.02 atom % (mean \pm SD). Additionally, 1 mL of $H^{13}CO_3$
121 (1g/50 mL) (Sigma- Aldrich, Saint Louis Missouri US) was added to each incubation bottle, roughly corresponding to 10
122 atom % enrichment and thus measurements of primary production and N₂ fixation were conducted in the same bottle.
123 Following the addition of both isotopic components, the bottles were closed airtight with septa-fitted caps and incubated for
124 24 hours on-deck incubators with a continuous surface seawater flow. These incubators, partially shaded (using daylight-
125 filtering foil) to simulate in situ photosynthetically active radiation (PAR) conditions, aimed to replicate environmental
126 parameters experienced at the sampled depths. Control incubations utilizing atmospheric air served as controls to monitor
127 any natural changes in δ ¹⁵N not attributable to ¹⁵N-N₂ addition. These control incubations were conducted using the
128 dissolution method, like the ¹⁵N-N₂ enrichment experiments, but with the substitution of atmospheric air instead of isotopic
129 tracer.

130 After the incubation period, subsamples for nutrient analysis were taken from each incubation sample, and the remaining
131 content was subjected to the filtration process and were gently filtered (200 mbar) onto precombusted GF/F filters
132 (Advantec,

133 47 mm ϕ , 0.7 μ m nominal pore size). This step ensured a comprehensive examination of both nutrient dynamics and the
134 isotopic composition of the particulate pool in the incubated samples. Samples were stored at -20 °C until further analysis.
135 Upon arrival in the lab, the filters were dried at 60 °C and to eliminate particulate inorganic carbon, subsequently subject
136 to acid fuming during which they were exposed to concentrated hydrochloric acid (HCl) vapors overnight in a desiccator.
137

138 After undergoing acid treatment, the filters were carefully dried, then placed into tin capsules and pelletized for subsequent
139 analysis. The determination of POC and PON, as well as isotopic composition ($\delta^{13}\text{C}$ POC / $\delta^{15}\text{N}$ PON), was carried out
140 using an elemental analyzer (Flash EA, ThermoFisher, USA) connected to a mass spectrometer (Delta V Advantage Isotope
141 Ratio MS, ThermoFisher, USA) with the ConFlo IV interface. This analytical setup was applied to all filters. These values,
142 derived from triplicate incubation measurements, exhibited no omission of data points or identification of outliers. Final rate
143 calculations for N_2 fixation rates were performed after Mohr et al. (2010) and primary production rates after Slawyk et al.
144 (1977).

145 **2.3 Molecular methods**

146 The filters were flash-frozen in liquid nitrogen, crushed and DNA was extracted using the Qiagen DNA/RNA AllPrep Kit
147 (Qi-agen, Hildesheim, DE), following the procedure outlined by the manufacturer. The concentration and quality of the
148 extracted DNA was assessed spectrophotometrically using a MySpec spectrofluorometer (VWR, Darmstadt, Germany).
149 The preparation of the metagenome library and sequencing were performed by BGI (China). Sequencing libraries were
150 generated using MGIEasy Fast FS DNA Library Prep Set following the manufacturer's protocol. Sequencing was
151 conducted with 2x150bp on a DNBSEQ-G400 platform (MGI). SOAPnuke1.5.5 (Chen et al. (2018)) was used to filter
152 and trim low quality reads and adaptor contaminants from the raw sequence reads, as clean reads. In total, fifteen
153 metagenomic datasets were produced with an average of 9.6G bp per sample.

155 **2.3.1 Metagenomic De Novo assembly, gene prediction, and annotation**

156 Megahit v1.2.9 (Li et al. (2015)) was used to assemble clean reads for each dataset with its minimum contig length as 500.
157 Prodigal v2.6.3 (Hyatt et al. (2010)) with the setting of “-p meta” was then used to predict the open reading frames (ORFs)
158 of the assembled contigs. ORFs from all the available datasets were filtered (>100bp), dereplicated and merged into a
159 catalog of non-redundant genes using cd-hit-est (>95 % sequence identity) (Fu et al. (2012)). Salmon v1.10.0 (Patro et al.
160 (2017)) with the “- meta” option was employed to map clean reads of each dataset to the catalog of non-redundant genes
161 and generate the GPM (genes per million reads) abundance. EggNOG mapper v2.1.12 (Cantalapiedra et al. (2021)) was then
162 performed to assign KEGG Orthology (KO) and identify specific functional annotation for the catalog of non-redundant
163 genes. The marker genes, *nifDK* (K02586, K02591 nitrogenase molybdenum-iron protein alpha/beta chain) and *nifH*
164 (K02588, nitrogenase iron protein), were used for the evaluation of microbial potential of N_2 fixation. *RbcL* (K01601,
165 ribulose-bisphosphate carboxylase large chain) and *psbA* (K02703, photosystem II P680 reaction center D1 protein) were
166 selected to evaluate the microbial potential of carbon fixation and photosynthesis, respectively. The molecular datasets
167 have been deposited with the accession number: Bioproject PRJNA1133027.

169 **3 Results and discussion**

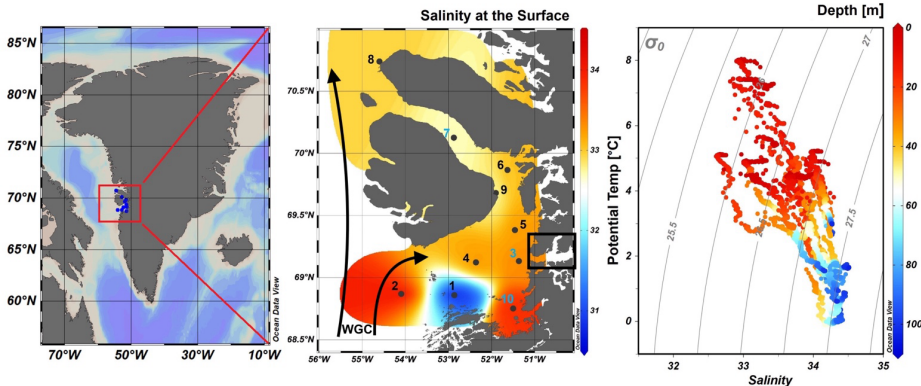
170 **3.1 Hydrographic conditions in Qeqertarsuaq (Disco Bay) and Sullorsuaq (Vaigat) Strait**

Field Code Changed

Field Code Changed

172
173 Disko Bay (Qeqertarsuaq) is located along the west coast of Greenland (Kalaallit Nunaat) at approximately 69 °N (Figure
174 1), and is strongly influenced by the West Greenland Current (WGC) which is associated with the broader Baffin Bay Polar
175 Waters (BBPW) (Mortensen et al., 2022; Hansen et al., 2012). The WGC does not only significantly shape the hydrographic
176 conditions within the bay but also plays an important role in the larger context of Greenland Ice Sheet melting (Mortensen
177 et al. (2022)). Central to the hydrographic system of the Qeqertarsuaq area is the Jakobshavn Isbræ, which is the most
178 productive glacier in the northern hemisphere and believed to drain about 7 % of the Greenland Ice Sheet and thus
179 contributes substantially to the water influx into the Qeqertarsuaq (Holland et al. (2008)). A predicted increased inflow of
180 warm subsurface water, originating from North Atlantic waters, has been suggested to further affect the melting of the
181 Jakobshavn Isbræ and thus adds another layer of complexity to this dynamic system (Holland et al., 2008; Hansen et al.,
182 2012).

183 The hydrographic conditions in Qeqertarsuaq have a significant influence on biological processes, nutrient availability, and the



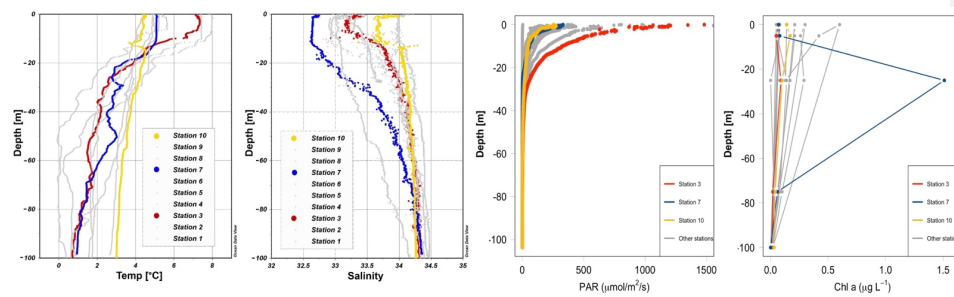
184
185 **Figure 1.** Map of Greenland (Kalaallit Nunaat) with indication of study area (red box), on the left. Interpolated distribution of Sea
186 Surface Salinity (SSS) values with corresponding isosurface lines and indication of 10 sampled stations (normal stations in black,
187 incubation stations in blue), black arrows indicate the West Greenland Current (WGC) and the black box indicate the location of the
188 Jakobshavn Isbræ, in the middle. Scatterplot of the potential temperature and salinity for all station data. The plot is used for the
189 identification of the main water masses within the study area. Isopycnals (kg m^{-3}) are depicted in grey lines, on the right. Figures were
190 created in Ocean Data View (ODV) (Schlitzer (2022)).

191 broader marine ecosystem (Munk et al., 2015; Hendry et al., 2019; Schiøtt, 2023).

193 During our survey, we found very heterogenous hydrographic conditions at the different stations across Qeqertarsuaq (Fig.
194 1 & Fig. 2). The three selected stations for N₂ fixation analysis (stations 3, 7, and 10) were strategically chosen to capture the

195 spatial

196 variability of the area. Surface salinity and temperature measurements at these stations indicate the influence of freshwater
197 input. The surface temperature exhibit a range of 4.5 to 8 °C, while surface salinity varies between 31 and 34, as illustrated
198 in Fig. 1. The profiles sampled during our survey extend to a maximum depth of 100 m. Comparison of temperature/salinity
199 (T/S) plots with recent studies suggests the presence of previously described water masses, including Warm Fjord Water
200 (WFjW) and Cold Fjord Water (CFjW) with an overlaying surface glacial meltwater runoff. Those water masses are defined
201 with a density range of $27.20 \leq \sigma_0 \leq 27.31$ but different temperature profiles. Thus water masses can be differentiated by
202 their temperature within the same density range (Gladish et al. (2015)). Other water masses like upper subpolar mode water
203 (uSPMW), deep subpolar mode water (dSPMW) and Baffin Bay polar Water (BBPW) which has been identified in the
204 Disko Bay (Qeqertarsuaq) before, cannot be identified from this data and may be present in deeper layers (Mortensen et
205 al., 2022; Sherwood et al., 2021; Myers and Ribergaard, 2013; Rysgaard et al., 2020). The temperature and salinity profiles
206 across the 10



207
208
209
210 **Figure 2.** Profiles of temperature (°C), salinity, photosynthetically active radiation (PAR) ($\mu\text{mol}/\text{m}^2/\text{s}$) and Chl a (mg m^{-3}) across stations
211 1 to 10 with depth (m). Stations 3, 7, and 10 are highlighted in red, blue, and yellow, respectively, to emphasize incubation stations.
212 Figures were created in Ocean Data View and R-Studio (Schlitzer (2022)).

213 stations in the study area show distinct stratification and variability, which is represented through the three incubation
214 stations (highlighted stations 3, 7, and 10 in Fig. 2). They display varying degrees of stratification and mixing, with notable
215 differences in the salinity and temperature profiles. Station 3 and station 7 exhibit clear stratification in both temperature
216 and salinity marked by the presence of thermoclines and haloclines. These features suggest significant freshwater input
217 influenced by local weather conditions and climate dynamics, like surface heat absorption. In contrast, Station 10 exhibits a
218 narrower range of temperature and salinity values throughout the water column compared to Stations 3 and 7, indicating
219 more well-mixed conditions. This uniformity is likely influenced by the regional circulation pattern and partial upwelling
220 (Hansen et al., 2012; Krawczyk et al., 2022). The distinct characteristics observed at station 10, as illustrated in the surface
221

222 plot (Fig. 1), show an elevated salinity and colder temperatures compared
223 to the other stations. This feature suggests upwelling of deeper waters along the shallower shelf, likely facilitated by the
224 local seafloor topography. Specifically, the seafloor shallowing off the coast of Station 10 may act as a barrier, disrupting
225 typical circulation and forcing deeper, saltier, and colder waters to the surface. This pattern aligns with previous studies that
226 describe similar mechanisms in the region (Krawczyk et al. (2022)). Their description of the bathymetry in Qeqertarsuaq,
227 featuring depths ranging from ca. 50 to 900 m, suggests its impact on turbulent circulation patterns, leading to the mixing
228 of different water masses. Evident variability in oceanographic conditions that can be observed throughout the study area
229 occurs particularly along characteristic topographical features like steep slopes, canyons, and shallower areas. The summer
230 melting of sea ice and glaciers introduces freshwater influxes that create distinct vertical and horizontal gradients in salinity
231 and temperature in the Qeqertarsuaq area Hansen et al. (2012). Additionally, the accelerated melting of the Jakobshavn
232 Isbraæ, influenced by the warmer inflow from the West Greenland Intermediate Current (WGIC), further alters the
233 hydrographic conditions. Recent observations indicate significant warming and shoaling of the WGIC, potentially enabling
234 it to overcome the sill separating the Ilulissat Fjord from the Qeqertarsuaq area (Hansen et al., 2012; Holland et al., 2008;
235 Myers and Ribergaard, 2013). This shift intensifies glacier melting, driving substantial changes in the local ecological
236 dynamics (Ardyna et al., 2014; Arrigo et al., 2008; Bhatia et al., 2013).

237 3.2 Elevated N₂ fixation rates might play a role in nutrient dynamics and bloom development

238 We quantified N₂ fixation rates within the waters of Qeqertarsuaq, spanning from the surface to a depth of 50 m (Table 1).
239 The rates ranged from 0.16 to 2.71 nmol N L⁻¹ d⁻¹ with all rates surpassing the detection limit. Our findings represent
240 rates at the upper range of those observed in the Arctic Ocean. Previous measurements in the region have been limited,
241 with only one study in Baffin Bay by Blais et al. (2012), reporting rates of 0.02 nmol N L⁻¹ d⁻¹, which are 1-2 orders of
242 magnitude lower than our observations. Moreover, Sipler et al. (2017), reported rates in the coastal Chukchi Sea, with
243 average values of 7.7 nmol N L⁻¹ d⁻¹. These values currently represent some of the highest rates measured in Arctic shelf
244 environments. Compared to these, our highest measured rate (2.71 nmol N L⁻¹ d⁻¹) is slower, but still substantial,
245 particularly considering the more Atlantic-influenced location of our study site. Sipler et al. (2017) also noted that a
246 significant fraction of diazotrophs were <3 μ m in size, suggesting that small unicellular diazotrophs play a dominant role
247 in Arctic nitrogen fixation. Altogether, our data contribute to the growing evidence that N₂ fixation is a widespread and
248 potentially significant nitrogen source across various Arctic regions. Simultaneous primary production rate measurements
249 ranged from 0.07 to 3.79 μ mol N L⁻¹ d⁻¹, with the highest rates observed at station 7 and generally higher values in the surface
250 layers. Employing Redfield stoichiometry, the measured N₂ fixation rates accounted for 0.47 to 2.6 % (averaging 1.57 %) of
251 primary production at our stations. The modest contribution to primary production suggests that N₂ fixation does not exert
252 a substantial influence on the productivity of these waters during the time of the sampling. Rather, our N₂ fixation rates
253 suggest primary production to depend mostly on additional nitrogen sources including regenerated, meltwater or ~~land-based~~
254 sources.

Deleted: land based

257 While the N:P ratio is commonly used to assess nutrient limitations relative to Redfield stoichiometry, most DIN and DIP
 258 measurements in our study were below detection limit (BDL), preventing a reliable calculation for this ratio. As such, we
 259 refrain from drawing conclusions based on N:P stoichiometry. Nevertheless, previous studies, by Jensen et al. (1999) and
 260 Tremblay and Gagnon (2009), have identified nitrogen limitation in this region. Such biogeochemical conditions, when present,
 261 would be expected to generate a niche for N₂ fixing organisms (Sohm et al. (2011)).
 262 While N₂ fixation did not chiefly sustain primary production during our sampling campaign, we hypothesize that N₂ fixation
 263 has the potential to play a role in bloom dynamics. As nitrogen availability decreases

264 during a bloom, it may provide a niche for N₂ fixation, potentially extending the productive period of the bloom (Reeder et
 265 al. (2021)). Satellite data indicates that a fall bloom began in early August, following the annual spring bloom, as described
 266 by Ardyna et al. (2014). This double bloom situation may be driven by increased melting and the subsequent input of
 267 bioavailable nutrients and iron (Fe) from meltwater runoff (Arrigo et al., 2017; Hopwood et al., 2016; Bhatia et al., 2013).
 268 The meltwater from the Greenland Ice Sheet is a significant source of Fe (Bhatia et al., 2013; Hawkings et al., 2015, 2014),
 269 which is a limiting factor especially for diazotrophs (Sohm et al. (2011)). Consequently, it is possible that nutrients and Fe
 270 from the Isbræ glacier introduced into the Qeqertarsuaq are promoting a bloom and further provide a niche for diazotrophs
 271 to thrive (Arrigo et al. (2017)).

272
 273
 274 **Table 1.** N₂ fixation (nmol N L⁻¹ d⁻¹), standard deviation (SD), primary productivity (PP; $\mu\text{mol C L}^{-1} \text{d}^{-1}$), SD, percentage of estimated
 275 new primary productivity (% New PP) sustained by N₂ fixation, dissolved inorganic nitrogen compounds (NO_x), phosphorus (PO₄) at
 276 stations 3, 7, and 10. BDL = Below detection limit.
 277

Station (no.)	Depth (m)	N ₂ fixation (nmol N L ⁻¹ d ⁻¹)	SD (\pm)	Primary Productivity ($\mu\text{mol C L}^{-1} \text{d}^{-1}$)	SD (\pm)	% New PP (%)	NO _x ($\mu\text{mol L}^{-1} \text{d}^{-1}$)	PO ₄ ($\mu\text{mol L}^{-1} \text{d}^{-1}$)
3	0	1.20	0.21	0.466	0.08	1.71	BDL	BDL
3	25	1.88	0.11	0.588	0.04	2.11	BDL	0.70
3	50	0.29	0.01	0.209	0.00	0.91	0.33	1.48
7	0	2.49	0.44	0.63	0.20	2.60	BDL	BDL
7	25	2.71	0.22	3.79	2.45	0.47	BDL	0.45
7	50	0.53	0.24	0.33	0.36	1.08	BDL	0.97
10	0	1.48	0.12	0.74	0.15	1.33	BDL	BDL
10	25	0.31	0.01	0.29	0.07	0.73	BDL	BDL
10	50	0.16	0	0.07	0.07	1.40	BDL	BDL

278 A near-Redfield stoichiometry in POC:PON suggests that the particulate organic matter (POM) likely originates from an
 279

Deleted: The N:P ratio, calculated as DIN to DIP, indicates a deficit in N for primary production based on Redfield stoichiometry (Fig. 3).

Deleted: This aligns with findings presented

Deleted: who observed a similar nitro- gen limitation

Deleted: -

Deleted: , and the molar nitrogen-to-phosphorus ratio (N:P)

Deleted: 0

Deleted: indicates

Deleted: is freshly derived

302 ongoing phytoplankton bloom, as phytoplankton generally assimilate carbon and nitrogen in relatively consistent
303 proportions during active growth (Redfield 1934). However this assumption is based on a global average, and POM
304 stoichiometry can exhibit substantial latitudinal variation. Deviations may also arise during particle production and
305 remineralization processes (Redfield 1934; Geider and La Roche 2002; Sterner and Elser 2017; Quigg et al., 2003). Recent
306 studies have further shown that POM composition vary widely across plankton communities, influenced by factors such
307 as growth rates, community composition, and physiological status (e.g. fast- vs- slow-growing organisms), with degradation
308 often playing a secondary role (Tanioka et al., 2022). Additionally, terrestrial organic material—likely introduced via
309 glacial outflow in the study area—may also contribute to the observed POM composition (Schneider et al., 2003).
310 Latitudinal variability in organic matter stoichiometry has also been linked to differences in nutrient supply and phosphorus
311 stress (Fagan et al., 2024; Tanioka et al., 2022). Consequently, the near-Redfield stoichiometry observed here cannot be
312 clearly attributed to freshly produced organic material. Nevertheless, satellite-derived surface chlorophyll *a* concentrations
313 and associated primary production support the interpretation that recently produced organic matter does contribute, at least
314 in part, to the sinking POM captured in our samples. Since inorganic nitrogen species (e.g., NO_x) were below detection
315 limits, direct calculation or interpretation of the N:P ratio in the dissolved nutrient pool was not possible and has been
316 avoided. The absence of available nitrogen may nonetheless reflect nitrogen depletion, potentially creating ecological
317 niches for diazotrophs and nitrogen-fixing organisms. Such conditions may promote shifts in microbial community
318 structure, as observed by Laso-Perez et al. (2024). Laso Perez et al. (2024) documented changes in microbial community
319 composition during an Arctic bloom, focusing on nitrogen cycling. They observed a shift from chemolithotrophic to
320 heterotrophic organisms throughout the summer bloom and noted increased activity to compete for various nitrogen sources.
321 However, no *nifH* gene copies, indicative of nitrogen-fixing organisms, were found in their dataset based on metagenome-
322 assembled genomes (MAGs). This is not unexpected due to the classically low abundance of diazotrophs in marine
323 microbial communities which has often been described (Turk-Kubo et al., 2015; Farnelid et al., 2019). Given the high
324 productivity and metabolic activity observed in Qeqertarsuaq during a similar bloom period, the detected diazotrophs
325 (Section 3.3) may play a more significant role than previously thought. Across the 10 stations there is considerable
326 variability in POC and PON concentrations (Fig. 3). PON concentrations range from 0.0 $\mu\text{mol N L}^{-1}$ to 3.48 $\mu\text{mol N L}^{-1}$
327 (n=124), while POC concentrations range from 2.7 $\mu\text{mol C L}^{-1}$ to 27.2 $\mu\text{mol C L}^{-1}$ (n=144). The highest concentrations for
328 both PON and POC were observed at station 7 at a depth of 25 m and coincide with the highest reported N₂ fixation rate
329 (Figure Appendix A2 & A3). Generally, POC and PON concentrations decrease with depth, peaking at the deep chl *a*
330 maximum (DCM), identified between 15 to 30 m across all stations. The DCM was identified based on measured chl *a*
331 concentrations and previous descriptions in the region (Fox and Walker, 2022; Jensen et al., 1999). The variability in chl *a*
332 concentrations indicates differences in phytoplankton abundance among the stations, with concentrations ranging between
333 0 to 0.42 mg m⁻³. Excluding station 7, which exhibited the highest chl *a* concentration at the DCM (1.51 mg m⁻³). While
334 Tang et al. (2019) found that N₂ fixation measurements strongly correlated to satellite estimates of chl *a* concentrations, our
335 results did not show a statistically significant correlation between nitrogen fixation rates and chl *a* concentrations overall

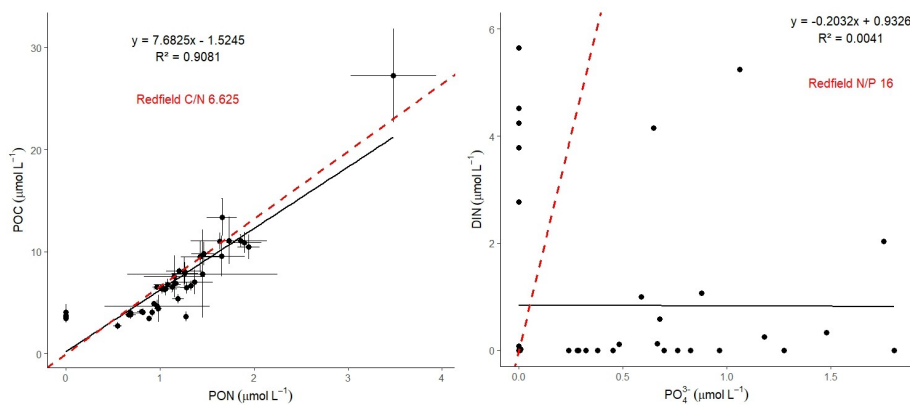
Deleted: In contrast, deviations from the Redfield ratio (e.g., elevated C:N or C:P) typically indicate microbial degradation and preferential remineralization of nitrogen and phosphorus (Redfield 1934; Geider and La Roche 2002; Sterner and Elser 2017).

Formatted: Font: Italic

Deleted: The absence of NO_x and the observed low N:P ratios suggest that nitrogen from earlier bloom phases has been largely depleted, potentially creating a niche for N₂ fixation as a supplementary nitrogen source. The onset and development of the bloom would be expected to lead to high nitrogen demands and intense competition for nitrogen sources. Notably, despite the apparent balance in the POM pool, the N:P ratio indicates strong nitrogen depletion and nutrient exhaustion within the ecosystem. This deficiency can be partly alleviated by N₂ fixation, providing possibly increasing amounts of nitrogen over the course of the bloom. Moreover, DIP is generally limited in the environment (Table 1); however, some organisms may still access it through luxury phosphorus uptake, storing excess phosphate when it is sporadically available. A recent study by ...

357 (Figures A2 & A3). However, as noted, Station 7 at 25 m represents a unique case. The elevated concentration of chl *a* at
 358 this station likely resulted from a local phytoplankton bloom induced by meltwater outflow from the Isbræ glacier and sea
 359 ice melting, which may help explain the observed nitrogen fixation rates (Arrigo et al., 2017; Wang et al., 2014). This
 360 study's findings are in agreement with prior reports of analogous blooms occurring in the region (Fox and Walker, 2022;
 361 Jensen et al., 1999).

362 Formatted: Font: Italic



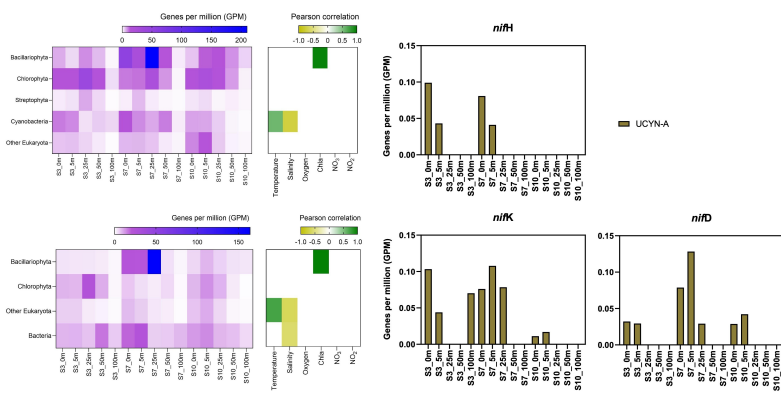
363
 364 **Figure 3.** The POC/PON and DIN/DIP ratios at all 10 stations. The red line represents the Redfield ratios of POC/PON (106:16) and
 365 DIN/DIP (16:1).
 366

367 3.3 Potential Contribution of UCYN-A to Nitrogen Fixation During a Diatom Bloom: Insights and Uncertainties

368 In our metagenomic analysis, we filtered the *nifH*, *nifD*, *nifK* genes, which code for the nitrogenase enzyme responsible
 369 for catalyzing N_2 fixation. We could identify sequences related to UCYN-A, which dominated the sequence pool of
 370 diazotrophs, particularly in the upper water masses (0 to 5 m) (Fig. 4). UCYN-A, a unicellular cyanobacterial symbiont, has
 371 a cosmopolitan distribution and is thought to substantially contribute to global N_2 fixation, as documented by (Martínez-
 372 Pérez et al., 2016; Tang et al., 2019). This conclusion is based on our metagenomic analysis, in which we set a sequence
 373 identity threshold of 95% for both *nif* and photosystem genes. Notably, we only recovered sequences related to UCYN-A
 374 within our *nif* sequence pool, suggesting its predominance among detected diazotrophs. However, metagenomic
 375 approaches may underestimate overall diazotroph diversity, and we cannot fully exclude the presence of other, less
 376 abundant diazotrophs that may have been missed using this method. While UCYN-A was primarily detected in surface
 377 waters, we also observed relatively high *nifK* values at S3_100m, an unusual finding given that UCYN-A is typically
 378

379 constrained to the euphotic zone. Previous studies have predominantly reported UCYN-A in surface waters; for instance
380 Harding et al. (2018) and Shiozaki et al. (2017) detected UCYN-A exclusively in the upper layers of the Arctic Ocean.
381 Additionally, Shiozaki et al. (2020) found UCYN-A2 at depths extending to the 0.1% light level but not below 66 m in the
382 Chukchi Sea. The detection of UCYN-A at 100 m in our study suggests that alternative mechanisms, such as particle
383 association, vertical transport, or local environmental conditions, may facilitate its presence at depth. This warrants further
384 investigation into the potential processes enabling its occurrence below the euphotic zone.
385 Due to the lack of genes such as those encoding Photosystem II and Rubisco, UCYN-A plays a significant role within the
386 host cell and participates in fundamental cellular processes. Consequently it has evolved to become a closely integrated
387 component of the host cell. Very recent findings demonstrate that UCYN-A imports proteins encoded by the host genome
388 and has been described as an early form of N₂ fixing organelle termed a "Nitroplast" (Coale et al. (2024)).
389 Previous investigations document that they are critical for primary production, supplying up to 85% of the fixed nitrogen to
390 their haptophyte host (Martínez-Pérez et al. (2016)). In addition to its high contribution to primary production, studies have
391 shown that UCYN-A in high latitude waters fix similar amounts of N₂ per cell as in the tropical Atlantic Ocean, even in
392 nitrogen- replete waters (Harding et al., 2018; Shiozaki et al., 2020; Martínez-Pérez et al., 2016; Krupke et al., 2015; Mills
393 et al., 2020). However, estimating their contribution to N₂ fixation in our study is challenging, particularly since we detected
394 cyanobacteria only at the surface but observe significant N₂ fixation rates below 5 m. The diazotrophic community is often
395 underrepresented in metagenomic datasets due to the low abundance of nitrogenase gene copies, implying our data does
396 not present a complete picture. We suspect a more diverse diazotrophic community exists, with UCYN-A being a significant
397 contributor to N₂ fixation in Arctic waters. However, the exact proportion of its contribution requires further investigation.
398 The contribution of N₂ fixation to carbon fixation (as percent of PP) is relatively low, at the time of our study. We identified
399 genes such as *rbcL*, which encodes Rubisco, a key enzyme in the carbon fixation pathway and *psbA*, a gene encoding
400 Photosystem II, involved in light-driven electron transfer in photosynthesis, in our metagenomic dataset. The gene *rbcL* (for
401 the carbon fixation pathway) and the gene *psbA* (for primary producers) were used to track the community of photosynthetic
402 primary producers in our metagenomic dataset. At station 7, elevated carbon fixation rates are correlated with high diatom
403 (*Bacillariophyta*) abundance and increased chl *a* concentration (Fig. 4), suggesting the onset of a bloom, which is also
404 observable via satellite images (Appendix A1). We hypothesize that meltwater, carrying elevated nutrient and trace metal
405 concentrations, was rapidly transported away from the glacier through the Vaigat Strait by strong winds, leading to increased
406 productivity, as previously described by Fox and Walker (2022) & Jensen et al. (1999). The elevated diatom abundance and
407 primary production rates at station 7 coincide with the highest N₂ fixation rates, which could possibly point toward a possible
408 diatom-diazotroph symbiosis (Foster et al., 2022, 2011; Schvarcz et al., 2022). However, we did not detect a clear
409 diazotrophic signal directly associated with the diatoms in our metagenomic dataset, which might be due to generally
410 underrepresentation of diazotrophs in metagenomes due to low abundance or low sequencing coverage. To investigate
411 this further, we examined the taxonomic composition of *Bacillariophyta* at higher resolution. Among the various
412 abundant diatom genera, *Rhizosolenia* and *Chaetoceros* have been identified as symbiosis with diazotrophs (Grosse,

413 *et al.*, 2010; Foster, *et al.*, 2010), representing less than 6% or 15% of *Bacillariophyta*, based on *rbcL* or *psbA*,
 414 respectively (Figure Appendix A4). Although we underestimate diazotrophs to an extent, the presence of certain
 415 diatom-diazotroph symbiosis could help explain the high nitrogen fixation rates in the diatom bloom to a certain
 416 degree. Compilation of *nif* sequences identified from this study as well as homologous from their NCBI top hit were
 417 added in Table S1. However, we cannot tell if the diazotrophs belong to UCYN-A1 or UCYN-A2, or UCYN-A3.
 418 Based on the Pierella Karlusich *et al.* (2021), they generated clonal *nifH* sequences from Tara Oceans, which the
 419 length of *nifH* sequences is much shorter than the two *nifH* sequences we generated in our study. Also, the available
 420 UCYN-A2 or UCYN-A3 *nifH* sequences from NCBI were shorter than the two *nifH* sequences we generated.
 421 Therefore, it would be not accurate to assign the *nifH* sequences to either group under UCYN-A. Furthermore, not
 422 much information is available regarding the different groups of UCYN-A using marker genes of *nifD* and *nifK*.
 423



424
 425 **Figure 4.** Upper left image: *psbA* with correlation plot. Lower left image: *rbcL* with correlation plot. Right image: *nifH*, *nifD*, *nifK*
 426 genes per million reads in the metagenomic datasets. All figures display molecular data from metagenomic dataset for all sampled depth
 427 of station 3,7,10

428 There is evidence that UCYN-A have a higher Fe demand, with input through meltwater or river runoff potentially being
 429 advantageous to those organisms (Shiozaki *et al.*, 2017, 2018; Cheung *et al.*, 2022). Consequently, UCYN-A might play a
 430 more critical role in the future with increased Fe-rich meltwater runoff. UCYN-A can potentially fuel primary productivity
 431 by supplying nitrogen, especially with increased melting, nutrient inputs, and more light availability due to rising
 432 temperatures as- sociated with climate change. This predicted enhancement of primary productivity may contribute to the
 433 biological drawdown of CO₂, acting as a negative feedback mechanism. These projections are based on studies forecasting
 434

437 increased temperatures, melting, and resulting biogeochemical changes leading to higher primary productivity. However
438 large uncertainties make predictions very difficult and should be handled with care. Thus we can only hypothesize that
439 UCYN-A might be coupled to these dynamics by providing essential nitrogen.

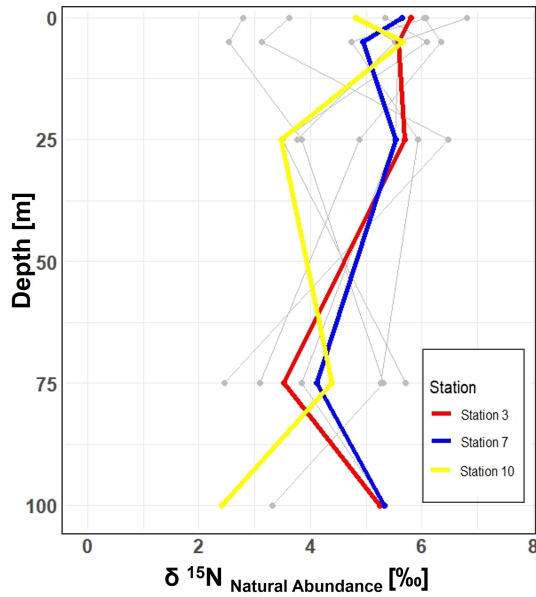
440 3.4 $\delta^{15}\text{N}$ Signatures in particulate organic nitrogen.

Deleted: show no clear evidence of nitrogen fixation

441 Stable isotopic composition, expressed using the $\delta^{15}\text{N}$ notation, serve as indicators for understanding nitrogen dynamics
442 because different biogeochemical processes fractionate nitrogen isotopes in distinct ways (Montoya (2008)). However, it
443 is important to keep in mind that the final isotopic signal is a combination of all processes and an accurate distinction
444 between processes cannot be made. N_2 fixation tends to enrich nitrogenous compounds with lighter isotopes, producing
445 OM with isotopic values ranging approximately from -2 to +2 ‰ (Dähnke and Thamdrup (2013)). Upon complete
446 remineralization and oxidation, organic matter contributes to a reduction in the average δ -values in the open ocean
447 (e.g. Montoya et al. (2002));

448 Emeis et al. (2010)). Whereas processes like denitrification and anammox preferentially remove lighter isotopes, leading
449 to enrichment in heavier isotopes and delta values up to -25 ‰.

450



453
454
455
456
457

Figure 5. Vertical profiles of $\delta^{15}\text{N}$ natural abundance signatures in PON across 10 stations in the study area. Incubation stations 3, 7, and 10 are highlighted in red, blue, and yellow, respectively. The figure shows variations in $\delta^{15}\text{N}$ signatures with depth at each station, providing insight into nitrogen cycling in the study area.

458
459
460
461
462
463
464
465

In our study, the $\delta^{15}\text{N}$ values of PON from all 10 stations, range between 2.45 ‰ and 8.30 ‰ within the 0 to 100 m depth range. While N_2 fixation typically produces OM ranging from -2 ‰ to 0.5 ‰, this signal can be masked by processes such as remineralization, mixing with nitrate from deeper waters or other biological transformations (Emeis et al. (2010); Sigman et al. (2009)). The composition of OM in the surface ocean is influenced by the nitrogen substrate and the fractionation factor during assimilation. When nitrate is depleted in the surface ocean, the isotopic signature of OM produced during photosynthesis will mirror that of the nitrogen source. Nitrate, the primary form of dissolved nitrogen in the open ocean, typically exhibits an average stable isotope value of around

466
467
468
469
470
471
472
473
474
475
476
477

5 ‰. No fractionation occurs during photosynthesis because the nitrogen source is entirely taken up in the surface waters (Sigman et al. (2009)). This matches conditions observed in Qeqertarsuaq, suggesting that subsurface nitrate is a dominant nitrogen source. (Fox and Walker (2022)). In the eastern Baffin Bay waters, Atlantic water masses serve as an important source of nitrate to surface waters, with $\delta^{15}\text{N}$ values around 5 ‰ (Sherwood et al. (2021)). This is consistent with our observed PON values and supports the view that primary productivity in the region is largely fueled by nitrate input from deeper Atlantic waters, particularly during early bloom stages. (Fox and Walker, 2022; Knies, 2022). The mechanisms through which subsurface nitrate reaches the euphotic layer are not well understood. However, potential pathways include vertical migration of phytoplankton and physical mixing. Subsequently, nitrogen undergoes rapid recycling and remineralization processes to meet the system's nitrogen demands (Jensen et al. (1999)). Taken together, the $\delta^{15}\text{N}$ signatures observed in this study are best interpreted as indicative of a system influenced by multiple nitrogen sources and biogeochemical processes, where nitrate input and remineralization appear to dominate.

478
479
480
481
482
483
484
485
486
487

4 Conclusion

Our study highlights the occurrence of elevated rates of N_2 fixation in Arctic coastal waters, particularly prominent at station 7, where they coincide with high chl *a* values, indicative of heightened productivity. Satellite observations tracing the origin of a bloom near the Isbræ Glacier, subsequently moving through the Vaigat strait, suggest a recurring phenomenon likely triggered by increased nutrient-rich meltwater originating from the glacier. This aligns with previous reports by Jensen et al. (1999) & Fox and Walker (2022), underlining the significance of such events in driving primary productivity in the region. The contribution of N_2 fixation to primary production was low (average 1.57 %) across the stations. Since the demand was high relative to the new nitrogen provided by N_2 fixation, the observed primary production must be sustained by the already

Deleted: Thus, $\delta^{15}\text{N}$ values help to identify different processes of the nitrogen cycle generally present in a system (Dähnke and Tham- drup (2013)).

Deleted: , thus do not exhibit a clear signal indicative of N_2 fixation. This suggests that N_2 fixation likely contributes only a certain fraction to export production or that it only started to contribute to isotope fractionation in the bloom dynamic.

Deleted: pho- tosynthesis

Deleted: substrate

Deleted: This substrate can originate from either nitrate in the subsurface or N_2 fixation.

Deleted: Notably,

Deleted: n

Deleted: In

Deleted: where similar conditions prevail, this

Deleted: s

Deleted: factors other than N_2 fixation are influencing the observed δ -values and POM is sustained by nitrogen sources from deeper subsurface waters, as observed in earlier studies.

Deleted: for sustaining primary produc- tivity

Deleted: , which is also reflected in the nitrogen isotopic signature in this study

Deleted: The influx of Atlantic waters, characterized by NO_3^- values of approximately 5 ‰, closely matches the $\delta^{15}\text{N}$ values of observed PON concentrations in our study. This suggests that Atlantic-derived NO_3^- serves as a primary source of new nitrogen to the initial stages of bloom development

518 present or adequate amount of subsurface supply of NO_x nutrients in the seawater. This is also visible in the isotopic signature
519 of the POM (Fox and Walker, 2022; Sherwood et al., 2021). However, the detected N_2 fixation rates are likely linked to the
520 development of the fresh secondary summer bloom, which could be sustained by high nutrient and Fe availability from
521 melting, potentially leading the system into a nutrient-limited state. The ongoing high demand for nitrogen compounds may
522 suggest an onset to further sustain the bloom, but it remains speculative whether Fe availability definitively contributes to
523 this process. The occurrence of such double blooms has increased by 10 % in the Qeqertarsuaq and even 33 % in the Baffin
524 Bay, with further projected increases moving north from Greenland (Kalaallit Nunaat) waters (Ardyna et al. (2014)). Thus,
525 nutrient demands are likely to increase, and the role of N_2 fixation can become more significant. The diazotrophic
526 community in this study is dominated by UCYN-A in surface waters and may be linked to diatom abundance in deeper
527 layers. This co-occurrence of diatoms and N_2 fixers in the same location is probably due to the co-limitation of similar
528 nutrients, rather than a symbiotic relationship. Thus, this highlights the significant presence of diazotrophs despite their
529 limited representation in datasets. It also highlights the potential for further discoveries, as existing datasets likely
530 underestimate the full extent of the diazotrophic community (Laso Perez et al., 2024);

531 [Shao et al., 2023](#); [Shiozaki et al., 2017, 2023](#)). The reported N_2 fixation rates in the Vaigat strait within the Arctic Ocean
532 are notably higher than those observed in many other oceanic regions, emphasizing that N_2 fixation is an active and
533 significant process in these high-latitude waters. When compared to measured rates across various ocean systems using the
534 ^{15}N approach, the significance of these findings becomes clear. For instance, N_2 fixation rates are sometimes below the
535 detection limit and often relatively low ranging from 0.8 to 4.4 nmol $\text{N L}^{-1} \text{d}^{-1}$ (Löscher et al., 2020, 2016; Turk et al., 2011).
536 In contrast, higher rates reach up to 20 nmol $\text{N L}^{-1} \text{d}^{-1}$ (Rees et al. (2009)) and sometime exceptional high rates range from
537 38 to 610 nmol $\text{N L}^{-1} \text{d}^{-1}$ (Bonnet et al. (2009)). The Arctic Ocean rates are thus significant in the global context,
538 underscoring the region's role in the global nitrogen cycle and the importance of N_2 fixation in supporting primary
539 productivity in these waters.

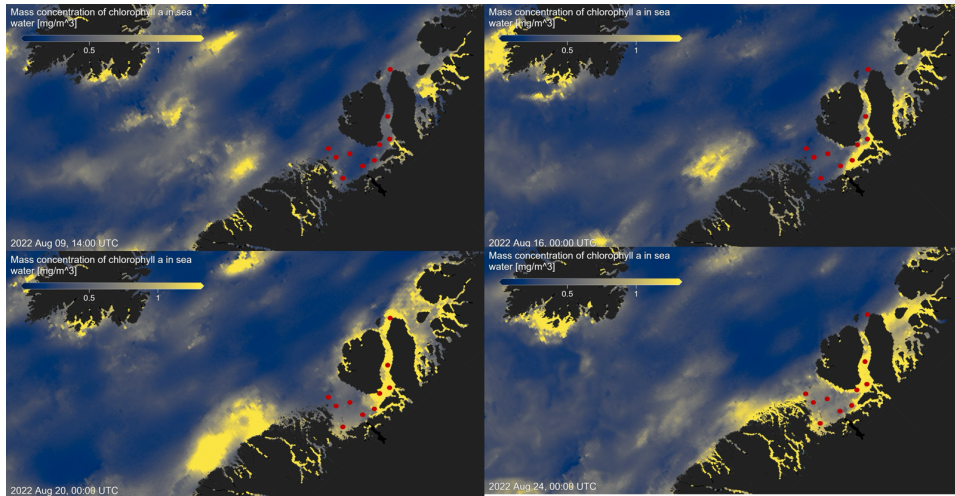
540 These findings highlight the urgent need to understand the interplay between seasonal variations, sea-ice dynamics, and
541 hydro- graphic conditions in Qeqertarsuaq. As climate change accelerates the melting of the Greenland Ice Sheet at
542 Jakobshavn Isbræ, shifts in hydrodynamic patterns and hydrographic conditions in Qeqertarsuaq are anticipated. The
543 resulting influx of warmer waters could significantly reshape the bay's hydrography, making it crucial to comprehend the
544 coupling of climate-driven changes and oceanic processes in this vital Arctic region. Our study provides key insights into
545 these dynamics and underscores the importance of continued investigation to predict Qeqertarsuaq's future hydrographic
546 state. By detailing the environmental and hydrographic changes, we contribute valuable knowledge to the broader context
547 of N_2 fixation in the Arctic Ocean. Given nitrogen's pivotal role in Arctic ecosystem productivity, it is essential to explore
548 diazotrophs, quantify N_2 fixation, and assess their impact on ecosystem services as climate change progresses.

549 **Appendix A**

550

551

Field Code Changed
Field Code Changed



552
553 **Figure A1.** Chlorophyll *a* concentration mg m^{-3} at four time points before, during, and after sea water sampling in August
554 2022 (sampling stations indicated by red dots), obtained from MODIS-Aqua; <https://giovanni.gsfc.nasa.gov> (Aqua MODIS Global
555 Mapped Chl *a* Data, version R2022.0, DOI:10.5067/AQUA/MODIS/L3M/CHL/2022), 4 km resolution, last access 03 June 2024

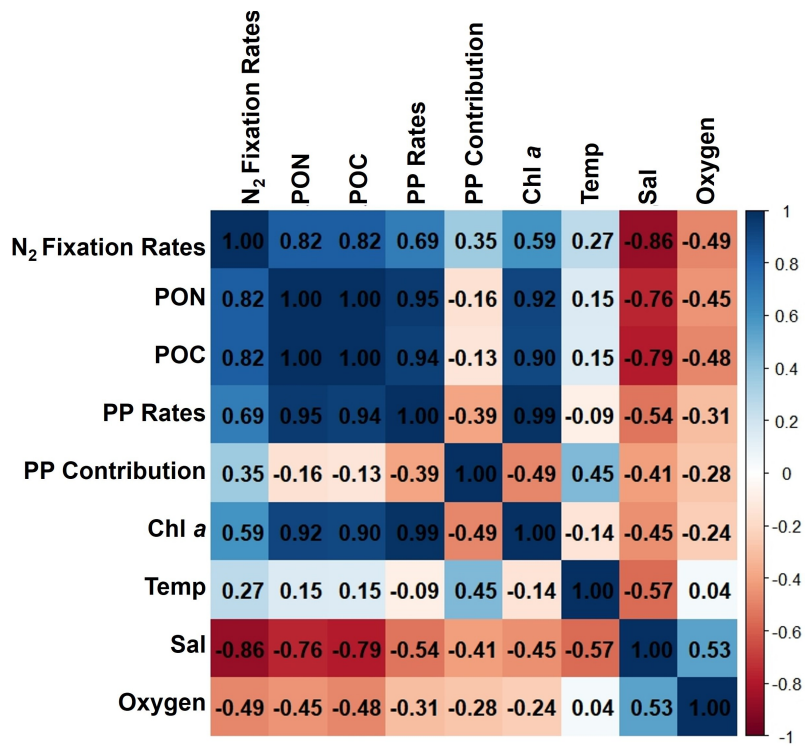
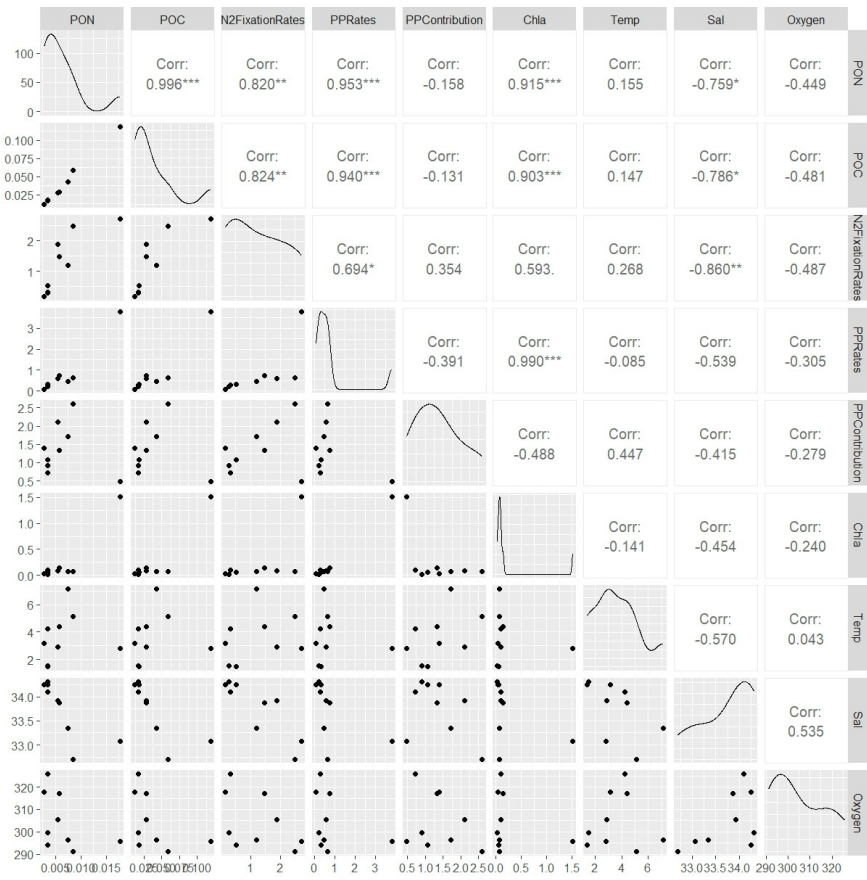
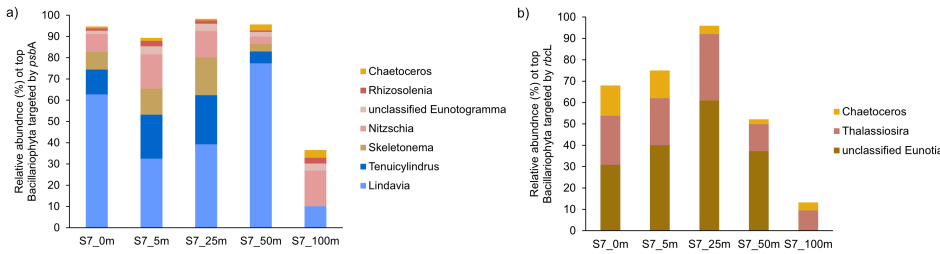


Figure A2. Correlation matrix of environmental and biological variables. The plot shows the correlation coefficients between the following parameters: N₂ fixation rates, PON, POC, PP rates, the contribution N₂ fixation to PP (PP contribution), Chl a, temperature (Temp), salinity (Sal), and Oxygen. The scale ranges from -1 to 1, where values close to 1 or -1 indicate strong positive or negative correlations, respectively, and values near 0 indicate weak or no correlation. The color intensity represents the strength and direction of the correlations, facilitating the identification of relationships among the variables



570
571
572



573
574 **Figure A4.** Taxonomic composition of Bacillariophyta at Station 7 based on a) psbA and b) rbcL marker genes. The figure shows the relative
575 abundance of Bacillariophyta genera detected in the metagenomic dataset, grouped by gene-specific classifications.

576

577

578

579

Data availability. The presented data collected during the cruise will be made accessible on PANGEA. The molecular datasets have been deposited with the accession number: Bioproject PRJNA1133027

580

581

582

583

Author contributions. IS carried out fieldwork and laboratory work at the University of Southern Denmark, and wrote the majority of the manuscript. ELP, AM, and EL conducted fieldwork and laboratory work at the University of Southern Denmark. PX performed metagenomic analysis and created the corresponding graphs. CRL designed the study, provided supervision and guidance throughout the project, and contributed to the writing and revision of the manuscript. All authors contributed to the conception of the study and participated in the writing and revision of the manuscript.

588

589

590

591

Competing interests. The authors declare that they have no known competing financial interests or personal relationships that could have appeared to influence the work reported in this paper. One of the authors, CRL, serves as an Associate Editor for Biogeosciences.

593

594

595

596

597

598

599

600

601

Acknowledgements. This work was supported by the Velux Foundation (grant no.29411 to Carolin R. Löscher) and through the DFF grant from the the Independent Research Fund Denmark (grant no. 0217-00089B to Lasse Riemann, Carolin R. Löscher and Stig Markager). ELP was supported by a postdoctoral contract from Danmarks Frie Forskningsfond (DFF, 1026-00428B) at SDU, and by a Marie Skłodowska- Curie postdoctoral fellowship (HORIZON2021 MSCA-2021-PF-01, project number: 101066750) by the European Commission at Princeton University. We sincerely thank the captain and crew of the P540 during the cruise on the Danish military vessel for their invaluable support and cooperation at sea. Our gratitude extends to Isaaffik Arctic Gateway for providing the infrastructure and

602 opportunities that made this project possible. We also acknowledge Zarah Kofoed for her technical support in the laboratory and thank all
603 the Nordceo laboratory technicians for their general assistance.

604 References

605

606 Ardyna, M. and Arrigo, K. R.: Phytoplankton dynamics in a changing Arctic Ocean, *Nature Climate Change*, 10, 892–903, 2020.

607 Ardyna, M., Babin, M., Gosselin, M., Devred, E., Rainville, L., and Tremblay, J.-É.: Recent Arctic Ocean sea ice loss triggers novel fall
608 phytoplankton blooms, *Geophysical Research Letters*, 41, 6207–6212, 2014.

609 Arrigo, K. R. and van Dijken, G. L.: Continued increases in Arctic Ocean primary production, *Progress in oceanography*, 136, 60–70,
610 2015. Arrigo, K. R., van Dijken, G., and Pabi, S.: Impact of a shrinking Arctic ice cover on marine primary production, *Geophysical
611 Research Letters*, 35, 2008.

612 Arrigo, K. R., van Dijken, G. L., Castelao, R. M., Luo, H., Rennermalm, Å. K., Tedesco, M., Mote, T. L., Oliver, H., and Yager, P. L.:
613 Melting glaciers stimulate large summer phytoplankton blooms in southwest Greenland waters, *Geophysical Research Letters*, 44,
614 6278–6285, 2017.

615 Bhatia, M. P., Kujawinski, E. B., Das, S. B., Breier, C. F., Henderson, P. B., and Charette, M. A.: Greenland meltwater as a significant
616 and potentially bioavailable source of iron to the ocean, *Nature Geoscience*, 6, 274–278, 2013.

617 Blais, M., Tremblay, J.-É., Jungblut, A. D., Gagnon, J., Martin, J., Thaler, M., and Lovejoy, C.: Nitrogen fixation and identification of
618 potential diazotrophs in the Canadian Arctic, *Global Biogeochemical Cycles*, 26, 2012.

619 Bonnet, S., Biegala, I. C., Dutrieux, P., Slemmons, L. O., and Capone, D. G.: Nitrogen fixation in the western equatorial Pacific: Rates,
620 diazotrophic cyanobacterial size class distribution, and biogeochemical significance, *Global Biogeochemical Cycles*, 23, 2009.

621 Buchanan, P. J., Chase, Z., Matear, R. J., Phipps, S. J., and Bindoff, N. L.: Marine nitrogen fixers mediate a low latitude pathway for
622 atmospheric CO₂ drawdown, *Nature Communications*, 10, 4611, 2019.

623 Cantalapiedra, C. P., Hernández-Plaza, A., Letunic, I., Bork, P., and Huerta-Cepas, J.: eggNOG-mapper v2: functional annotation,
624 orthology assignments, and domain prediction at the metagenomic scale, *Molecular biology and evolution*, 38, 5825–5829, 2021.

625 Capone, D. G. and Carpenter, E. J.: Nitrogen fixation in the marine environment, *Science*, 217, 1140–1142, 1982.

626 Chen, Y., Chen, Y., Shi, C., Huang, Z., Zhang, Y., Li, S., Li, Y., Ye, J., Yu, C., Li, Z., et al.: SOAPnuke: a MapReduce acceleration-
627 supported software for integrated quality control and preprocessing of high-throughput sequencing data, *Gigascience*, 7, gix120, 2018.

628 Cheung, S., Liu, K., Turk-Kubo, K. A., Nishioka, J., Suzuki, K., Landry, M. R., Zehr, J. P., Leung, S., Deng, L., and Liu, H.: High
629 biomass turnover rates of endosymbiotic nitrogen-fixing cyanobacteria in the western Bering Sea, *Limnology and Oceanography
630 Letters*, 7, 501–509, 2022.

631 Coale, T. H., Loconte, V., Turk-Kubo, K. A., Vanslembrouck, B., Mak, W. K. E., Cheung, S., Ekman, A., Chen, J.-H., Hagino, K.,
632 Takano, Y., et al.: Nitrogen-fixing organelle in a marine alga, *Science*, 384, 217–222, 2024.

633 Dähnke, K. and Thamdrup, B.: Nitrogen isotope dynamics and fractionation during sedimentary denitrification in Boknis Eck, Baltic
634 Sea, *Biogeosciences*, 10, 3079–3088, 2013.

635 Damm, E., Helmke, E., Thoms, S., Schauer, U., Nöthig, E., Bakker, K., and Kiene, R.: Methane production in aerobic oligotrophic
636 surface water in the central Arctic Ocean, *Biogeosciences*, 7, 1099–1108, 2010.

637 Diez, B., Bergman, B., Pedrós-Alió, C., Antó, M., and Snoeijis, P.: High cyanobacterial *nifH* gene diversity in Arctic seawater and sea
638 ice brine, *Environmental microbiology reports*, 4, 360–366, 2012.

639

640 Emeis, K.-C., Mara, P., Schlarbaum, T., Möbius, J., Dähnke, K., Struck, U., Mihalopoulos, N., and Krom, M.: External N inputs and
641 internal N cycling traced by isotope ratios of nitrate, dissolved reduced nitrogen, and particulate nitrogen in the eastern Mediterranean
642 Sea, *Journal of Geophysical Research: Biogeosciences*, 115, 2010.

643 Falkowski, P. G., Fenchel, T., and Delong, E. F.: The microbial engines that drive Earth's biogeochemical cycles, *science*, 320, 1034–
644 1039, 2008.

645 Farnelid, H., Andersson, A. F., Bertilsson, S., Al-Soud, W. A., Hansen, L. H., Sørensen, S., Steward, G. F., Hagström, Å., and Riemann,
646 L.: Nitrogenase gene amplicons from global marine surface waters are dominated by genes of non-cyanobacteria, *PLoS one*, 6, e19223,
647 2011.

648 Farnelid, H., Turk-Kubo, K., Ploug, H., Ossolinski, J. E., Collins, J. R., Van Mooy, B. A., and Zehr, J. P.: Diverse diazotrophs are present
649 on sinking particles in the North Pacific Subtropical Gyre, *The ISME journal*, 13, 170–182, 2019.

650 Fernández-Méndez, M., Turk-Kubo, K. A., Buttigieg, P. L., Rapp, J. Z., Krumpen, T., and Zehr, J. P.: Diazotroph diversity in the sea ice,
651 melt ponds, and surface waters of the Eurasian Basin of the Central Arctic Ocean, *Frontiers in microbiology*, 7, 217 140, 2016.

652 Foster, R. A., Goebel, N. L., & Zehr, J. P.: Isolation of calothrix rhizosoleniae (cyanobacteria) strain SC01 from *chaetoceros*
653 (bacillariophyta) spp. diatoms of the subtropical north pacific ocean 1. *Journal of Phycology*, 46(5), 1028–1037, 2010.

654 Foster, R. A., Kuypers, M. M., Vagner, T., Paerl, R. W., Musat, N., and Zehr, J. P.: Nitrogen fixation and transfer in open ocean
655 diatom–cyanobacterial symbioses, *The ISME journal*, 5, 1484–1493, 2011.

656 Foster, R. A., Tienken, D., Littmann, S., Whitehouse, M. J., Kuypers, M. M., and White, A. E.: The rate and fate of N2 and C fixation
657 by marine diatom–diazotroph symbioses, *The ISME journal*, 16, 477–487, 2022.

658 Fox, A. and Walker, B. D.: Sources and Cycling of Particulate Organic Matter in Baffin Bay: A Multi-Isotope $\delta^{13}\text{C}$, $\delta^{15}\text{N}$, and $\Delta^{14}\text{C}$
659 Approach, *Frontiers in Marine Science*, 9, 846 025, 2022.

660 Fu, L., Niu, B., Zhu, Z., Wu, S., and Cd-hit, W. L.: Accelerated for clustering the next-generation sequencing data, *Bioinformatics*,
661 28, 3150–3152, 2012.

662 Galloway, J., Dentener, F., Capone, D., Boyer, E., Howarth, R., Seitzinger, S., Asner, G., Cleveland, C., Green, P., Holland, E., et al.:
663 Nitrogen cycles: past, present, and future. *Biogeochemistry* 70, 153e226, 2004.

664 Garcia-Robledo, E., Corzo, A., and Papaspyrou, S.: A fast and direct spectrophotometric method for the sequential determination of
665 nitrate and nitrite at low concentrations in small volumes, *Marine Chemistry*, 162, 30–36, 2014.

666 Geider, R. J., & La Roche, J.: Redfield revisited: variability of C [ratio] N [ratio] P in marine microalgae and its biochemical
667 basis. *European Journal of Phycology*, 37(1), 1–17, 2002.

668 Gladish, C. V., Holland, D. M., and Lee, C. M.: Oceanic boundary conditions for Jakobshavn Glacier. Part II: Provenance and sources
669 of variability of Disko Bay and Ilulissat icefjord waters, 1990–2011, *Journal of Physical Oceanography*, 45, 33–63, 2015.

670 Grosse, J., Bombar, D., Doan, H. N., Nguyen, L. N., & Voss, M.: The Mekong River plume fuels nitrogen fixation and determines
671 phytoplankton species distribution in the South China Sea during low and high discharge season. *Limnology and
672 Oceanography*, 55(4), 1668–1680, 2010.

673 Großkopf, T., Mohr, W., Baustian, T., Schunck, H., Gill, D., Kuypers, M. M., Lavik, G., Schmitz, R. A., Wallace, D. W., and LaRoche,
674 J.: Doubling of marine dinitrogen-fixation rates based on direct measurements, *Nature*, 488, 361–364, 2012.

675 Gruber, N.: The dynamics of the marine nitrogen cycle and its influence on atmospheric CO₂ variations, in: *The ocean carbon cycle
676 and climate*, pp. 97–148, Springer, 2004.

677 Gruber, N. and Galloway, J. N.: An Earth-system perspective of the global nitrogen cycle, *Nature*, 451, 293–296, 2008.

678 Gruber, N. and Sarmiento, J. L.: Global patterns of marine nitrogen fixation and denitrification, *Global biogeochemical cycles*, 11, 235–
679 266, 1997.

680 Haine, T. W., Curry, B., Gerdes, R., Hansen, E., Karcher, M., Lee, C., Rudels, B., Spreen, G., de Steur, L., Stewart, K. D., et al.: Arctic
681 freshwater export: Status, mechanisms, and prospects, *Global and Planetary Change*, 125, 13–35, 2015.

682 Hanna, E., Huybrechts, P., Steffen, K., Cappelen, J., Huff, R., Shuman, C., Irvine-Fynn, T., Wise, S., and Griffiths, M.: Increased runoff
683 from melt from the Greenland Ice Sheet: a response to global warming, *Journal of Climate*, 21, 331–341, 2008.

684 Hansen, M. O., Nielsen, T. G., Stedmon, C. A., and Munk, P.: Oceanographic regime shift during 1997 in Disko Bay, western
685 Greenland, *Limnology and Oceanography*, 57, 634–644, 2012.

686 Harding, K., Turk-Kubo, K. A., Sipler, R. E., Mills, M. M., Bronk, D. A., and Zehr, J. P.: Symbiotic unicellular cyanobacteria fix nitrogen
687 in the Arctic Ocean, *Proceedings of the National Academy of Sciences*, 115, 13 371–13 375, 2018.

688 Hawkings, J., Wadham, J., Tranter, M., Lawson, E., Sole, A., Cowton, T., Tedstone, A., Bartholomew, I., Nienow, P., Chandler, D., et
689 al.: The effect of warming climate on nutrient and solute export from the Greenland Ice Sheet, *Geochemical Perspectives Letters*, pp.
690 94–104, 2015.

691 Hawkings, J. R., Wadham, J. L., Tranter, M., Raiswell, R., Benning, L. G., Statham, P. J., Tedstone, A., Nienow, P., Lee, K., and Telling,
692 J.: Ice sheets as a significant source of highly reactive nanoparticulate iron to the oceans, *Nature communications*, 5, 1–8, 2014.

693 Hendry, K. R., Huvenne, V. A., Robinson, L. F., Annett, A., Badger, M., Jacobel, A. W., Ng, H. C., Opher, J., Pickering, R. A., Taylor, M.
694 L., et al.: The biogeochemical impact of glacial meltwater from Southwest Greenland, *Progress in Oceanography*, 176, 102 126, 2019.

695 Holland, D. M., Thomas, R. H., De Young, B., Rønne, M. H., and Lyberth, B.: Acceleration of Jakobshavn Isbræ triggered by warm
696 subsurface ocean waters, *Nature geoscience*, 1, 659–664, 2008.

697 Hopwood, M. J., Connelly, D. P., Arendt, K. E., Juul-Pedersen, T., Stinchcombe, M. C., Meire, L., Esposito, M., and Krishna, R.:
698 Seasonal changes in Fe along a glaciated Greenlandic fjord, *Frontiers in Earth Science*, 4, 15, 2016.

699 Hyatt, D., Chen, G.-L., LoCascio, P. F., Land, M. L., Larimer, F. W., and Hauser, L. J.: Prodigal: prokaryotic gene recognition and
700 translation initiation site identification, *BMC bioinformatics*, 11, 1–11, 2010.

701 Jensen, H. M., Pedersen, L., Burmeister, A., and Winding Hansen, B.: Pelagic primary production during summer along 65 to 72 N off
702 West Greenland, *Polar Biology*, 21, 269–278, 1999.

703 Karl, D., Michaels, A., Bergman, B., Capone, D., Carpenter, E., Letelier, R., Lipschultz, F., Paerl, H., Sigman, D., and Stal, L.: Dinitrogen
704 fixation in the world's oceans, *The nitrogen cycle at regional to global scales*, pp. 47–98, 2002.

705 Knies, J.: Nitrogen isotope evidence for changing Arctic Ocean ventilation regimes during the Cenozoic, *Geophysical Research Letters*,
706 49, e2022GL099 512, 2022.

707 Krawczyk, D. W., Yesson, C., Knutz, P., Arboe, N. H., Blicher, M. E., Zinglerson, K. B., and Wagnholt, J. N.: Seafloor habitats across
708 geological boundaries in Disko Bay, central West Greenland, *Estuarine, Coastal and Shelf Science*, 278, 108 087, 2022.

709 Krupke, A., Mohr, W., LaRoche, J., Fuchs, B. M., Amann, R. I., and Kuypers, M. M.: The effect of nutrients on carbon and nitrogen
710 fixation by the UCYN-A–haptophyte symbiosis, *The ISME journal*, 9, 1635–1647, 2015.

711 Laso Perez, R., Rivas Santisteban, J., Fernandez-Gonzalez, N., Mundy, C. J., Tamames, J., and Pedros-Alio, C.: Nitrogen cycling during
712 an Arctic bloom: from chemolithotrophy to nitrogen assimilation, *bioRxiv*, pp. 2024–02, 2024.

713 Lewis, K., Van Dijken, G., and Arrigo, K. R.: Changes in phytoplankton concentration now drive increased Arctic Ocean primary

714 production, *Science*, 369, 198–202, 2020.

715 Li, D., Liu, C.-M., Luo, R., Sadakane, K., and Lam, T.-W.: MEGAHIT: an ultra-fast single-node solution for large and complex
716 metagenomics assembly via succinct de Bruijn graph, *Bioinformatics*, 31, 1674–1676, 2015.

717 Löscher, C. R., Bourbonnais, A., Dekaezemacker, J., Charoenpong, C. N., Altabet, M. A., Bange, H. W., Czeschel, R., Hoffmann, C.,
718 and Schmitz, R.: N₂ fixation in eddies of the eastern tropical South Pacific Ocean, *Biogeosciences*, 13, 2889–2899, 2016.

719 Löscher, C. R., Mohr, W., Bange, H. W., and Canfield, D. E.: No nitrogen fixation in the Bay of Bengal?, *Biogeosciences*, 17, 851–864,
720 2020.

721 Luo, Y.-W., Doney, S., Anderson, L., Benavides, M., Berman-Frank, I., Bode, A., Bonnet, S., Boström, K. H., Böttjer, D., Capone,
722 D., et al.: Database of diazotrophs in global ocean: abundance, biomass and nitrogen fixation rates, *Earth System Science Data*, 4, 47–73,
723 2012.

724 Martínez-Pérez, C., Mohr, W., Löscher, C. R., Dekaezemacker, J., Littmann, S., Yilmaz, P., Lehnen, N., Fuchs, B. M., Lavik, G.,
725 Schmitz,
726 R. A., et al.: The small unicellular diazotrophic symbiont, UCYN-A, is a key player in the marine nitrogen cycle, *Nature Microbiology*,
1, 1–7, 2016.

727 Mills, M. M., Turk-Kubo, K. A., van Dijken, G. L., Henke, B. A., Harding, K., Wilson, S. T., Arrigo, K. R., and Zehr, J. P.: Unusual
728 marine cyanobacteria/haptophyte symbiosis relies on N₂ fixation even in N-rich environments, *The ISME Journal*, 14, 2395–2406,
729 2020.

730 Mohr, W., Grosskopf, T., Wallace, D. W., and LaRoche, J.: Methodological underestimation of oceanic nitrogen fixation rates, *PloS one*,
731 5, e12 583, 2010.

732 Montoya, J. P.: Nitrogen stable isotopes in marine environments, *Nitrogen in the marine environment*, 2, 1277–1302, 2008.

733 Montoya, J. P., Carpenter, E. J., and Capone, D. G.: Nitrogen fixation and nitrogen isotope abundances in zooplankton of the oligotrophic
734 North Atlantic, *Limnology and Oceanography*, 47, 1617–1628, 2002.

735 Mortensen, J., Rysgaard, S., Winding, M., Juul-Pedersen, T., Arendt, K., Lund, H., Stuart-Lee, A., and Meire, L.: Multidecadal water
736 mass dynamics on the West Greenland Shelf, *Journal of Geophysical Research: Oceans*, 127, e2022JC018 724, 2022.

737 Munk, P., Nielsen, T. G., and Hansen, B. W.: Horizontal and vertical dynamics of zooplankton and larval fish communities during mid-
738 summer in Disko Bay, West Greenland, *Journal of Plankton Research*, 37, 554–570, 2015.

739 Murphy, J. and Riley, J. P.: A modified single solution method for the determination of phosphate in natural waters, *Analytica chimica
740 acta*, 27, 31–36, 1962.

741 Myers, P. G. and Ribergaard, M. H.: Warming of the polar water layer in Disko Bay and potential impact on Jakobshavn Isbrae, *Journal
742 of Physical Oceanography*, 43, 2629–2640, 2013.

743 Patro, R., Duggal, G., Love, M. I., Irizarry, R. A., and Kingsford, C.: Salmon provides fast and bias-aware quantification of transcript
744 expression, *Nature methods*, 14, 417–419, 2017.

745 Quigg, A., Finkel, Z.V., Irwin, A.J., Rosenthal, Y., Ho, T.Y., Reinfelder, J.R., Schofield, O., Morel, F.M. and Falkowski, P.G.: The
746 evolutionary inheritance of elemental stoichiometry in marine phytoplankton, *Nature*, 425(6955), pp.291-294, 2003.

747 Redfield, A. C.: On the proportions of organic derivatives in sea water and their relation to the composition of plankton (Vol. 1). Liverpool:
748 university press of liverpool, 1934.

749 Reeder, C. F., Stoltenberg, I., Javidpour, J., and Löscher, C. R.: Salinity as a key control on the diazotrophic community composition in
750 the Baltic Sea, *Ocean Science Discussions*, 2021, 1–30, 2021.

751 Rees, A. P., Gilbert, J. A., and Kelly-Gerreyn, B. A.: Nitrogen fixation in the western English Channel (NE Atlantic ocean), *Marine*

Formatted: Font: Not Italic

Formatted: Font: Not Italic

Formatted

752 Ecology Progress Series, 374, 7–12, 2009.

753 Rysgaard, S., Boone, W., Carlson, D., Sejr, M., Bendtsen, J., Juul-Pedersen, T., Lund, H., Meire, L., and Mortensen, J.: An updated view
754 on water masses on the pan-west Greenland continental shelf and their link to proglacial fjords, *Journal of Geophysical Research: Oceans*, 125, e2019JC015 564, 2020.

755 Schiøtt, S.: The Marine Ecosystem of Ilulissat Icefjord, Greenland, Ph.D. thesis, Department of Biology, Aarhus University, Denmark,
756 2023. Schlitzer, R.: Ocean data view, 2022.

757 Schneider, B., Schlitzer, R., Fischer, G. and Nöthig, E.M.: Depth-dependent elemental compositions of particulate organic matter (POM)
758 in the ocean, *Global Biogeochemical Cycles*, 17(2), 2003.

759 Schvarcz, C. R., Wilson, S. T., Caffin, M., Stancheva, R., Li, Q., Turk-Kubo, K. A., White, A. E., Karl, D. M., Zehr, J. P., and Steward, G.
760 F.: Overlooked and widespread pennate diatom-diazotroph symbioses in the sea, *Nature communications*, 13, 799, 2022.

761 Shao, Z., Xu, Y., Wang, H., Luo, W., Wang, L., Huang, Y., Agawin, N. S. R., Ahmed, A., Benavides, M., Bentzon-Tilia, M., et al.:
762 Global oceanic diazotroph database version 2 and elevated estimate of global N 2 fixation, *Earth System Science Data*, 15, 2023.

763 Sherwood, O. A., Davin, S. H., Lehmann, N., Buchwald, C., Edinger, E. N., Lehmann, M. F., and Kienast, M.: Stable isotope ratios in
764 seawater nitrate reflect the influence of Pacific water along the northwest Atlantic margin, *Biogeosciences*, 18, 4491–4510, 2021.

765 Shiozaki, T., Bombar, D., Riemann, L., Hashihama, F., Takeda, S., Yamaguchi, T., Ehama, M., Hamasaki, K., and Furuya, K.: Basin
766 scale variability of active diazotrophs and nitrogen fixation in the North Pacific, from the tropics to the subarctic Bering Sea, *Global Biogeochemical Cycles*, 31, 996–1009, 2017.

767 Shiozaki, T., Fujiwara, A., Ijichi, M., Harada, N., Nishino, S., Nishi, S., Nagata, T., and Hamasaki, K.: Diazotroph community structure
768 and the role of nitrogen fixation in the nitrogen cycle in the Chukchi Sea (western Arctic Ocean), *Limnology and Oceanography*, 63,
769 2191–2205, 2018.

770 Shiozaki, T., Fujiwara, A., Inomura, K., Hirose, Y., Hashihama, F., and Harada, N.: Biological nitrogen fixation detected under Antarctic
771 sea ice, *Nature geoscience*, 13, 729–732, 2020.

772 Shiozaki, T., Nishimura, Y., Yoshizawa, S., Takami, H., Hamasaki, K., Fujiwara, A., Nishino, S., and Harada, N.: Distribution and
773 survival strategies of endemic and cosmopolitan diazotrophs in the Arctic Ocean, *The ISME journal*, 17, 1340–1350, 2023.

774 Sigman, D. M., DiFiore, P. J., Hain, M. P., Deutsch, C., Wang, Y., Karl, D. M., Knapp, A. N., Lehmann, M. F., and Pantoja, S.: The
775 dual isotopes of deep nitrate as a constraint on the cycle and budget of oceanic fixed nitrogen, *Deep Sea Research Part I: Oceanographic Research Papers*, 56, 1419–1439, 2009.

776 Sipler, R. E., Gong, D., Baer, S. E., Sanderson, M. P., Roberts, Q. N., Mulholland, M. R., and Bronk, D. A.: Preliminary estimates of
777 the contribution of Arctic nitrogen fixation to the global nitrogen budget, *Limnology and Oceanography Letters*, 2, 159–166, 2017.

778 Slawyk, G., Collos, Y., and Auclair, J.-C.: The use of the 13C and 15N isotopes for the simultaneous measurement of carbon and nitrogen
779 turnover rates in marine phytoplankton 1, *Limnology and Oceanography*, 22, 925–932, 1977.

780 Sohm, J. A., Webb, E. A., and Capone, D. G.: Emerging patterns of marine nitrogen fixation, *Nature Reviews Microbiology*, 9, 499–
781 508, 2011.

782 Stern, R. W., & Elser, J. J. Ecological stoichiometry: the biology of elements from molecules to the biosphere. In *Ecological stoichiometry*.
783 Princeton university press, 2017.

784 Tanioka, T., Garcia, C.A., Larkin, A.A., Garcia, N.S., Fagan, A.J. and Martiny, A.C.: Global patterns and predictors of C: N: P in marine
785 ecosystems, *Communications Earth & Environment*, 3(1), p.271, 2022.

Formatted: Font: Not Italic

Formatted: Font: Not Italic

Formatted: Font: Not Italic

Formatted: Font: Not Italic

789 Tang, W., Wang, S., Fonseca-Batista, D., Dehairs, F., Gifford, S., Gonzalez, A. G., Gallinari, M., Planquette, H., Sarthou, G., and Cassar,
790 N.: Revisiting the distribution of oceanic N₂ fixation and estimating diazotrophic contribution to marine production, *Nature
791 communications*, 10, 831, 2019.

792 Tremblay, J.-É. and Gagnon, J.: The effects of irradiance and nutrient supply on the productivity of Arctic waters: a perspective on
793 climate change, in: *Influence of climate change on the changing arctic and sub-arctic conditions*, pp. 73–93, Springer, 2009.

794 Turk, K. A., Rees, A. P., Zehr, J. P., Pereira, N., Swift, P., Shelley, R., Lohan, M., Woodward, E. M. S., and Gilbert, J.: Nitrogen fixation
795 and nitrogenase (*nifH*) expression in tropical waters of the eastern North Atlantic, *The ISME journal*, 5, 1201–1212, 2011.

796 Turk-Kubo, K. A., Frank, I. E., Hogan, M. E., Desnues, A., Bonnet, S., and Zehr, J. P.: Diazotroph community succession during the
797 VAHINE mesocosm experiment (New Caledonia lagoon), *Biogeosciences*, 12, 7435–7452, 2015.

798 Von Friesen, L. W. and Riemann, L.: Nitrogen fixation in a changing Arctic Ocean: an overlooked source of nitrogen?, *Frontiers in
799 Microbiology*, 11, 596 426, 2020.

800 Wang, S., Bailey, D., Lindsay, K., Moore, J., and Holland, M.: Impact of sea ice on the marine iron cycle and phytoplankton productivity,
801 *Biogeosciences*, 11, 4713–4731, 2014.

802 Zehr, J. P. and Capone, D. G.: Changing perspectives in marine nitrogen fixation, *Science*, 368, eaay9514, 2020.